A Weft Knit Data Glove

Emmanuel Ayodele[1], Syed Ali Raza Zaidi[1], Jane Scott[2], Zhiqiang Zhang[1], Ali Hayajneh[3], Samson Shittu[4], Des McLernon[1]

***Abstract*—Rehabilitation of stoke survivors can be expedited by employing an exoskeleton. The exercises are designed such that both hands move in synergy. In this regard often motion capture data from the healthy hand is used to derive control behaviour for the exoskeleton. Therefore, data gloves can provide a low-cost solution for the motion capture of the joints in the hand. However, current data gloves are bulky, inaccurate or inconsistent. These disadvantages are inherited because the conventional design of a glove involves an external attachment that degrades overtime and causes inaccuracies. This paper presents a weft knit data glove whose sensors and support structure are manufactured in the same fabrication process thus removing the need for an external attachment. The glove is made by knitting multifilament conductive yarn and an elastomeric yarn using WholeGarment technology. Furthermore, we present a detailed electromechanical model of the sensors alongside its experimental validation. Additionally, the reliability of the glove is verified experimentally. Lastly, machine learning algorithms are implemented for classifying the posture of hand on the basis of sensor data histograms.**

***Index Terms*—Weft Knit Sensor, Data glove, Wearable, Electromechanical modelling, Classification.**

I. Introduction

A. Motivation

STROKE is one of the major causes of disabilities in adults. A major challenge most stroke survivors face is the loss of their motor skills, especially the individual finger movements in the hand [1], [2]. Although only 15% fully recover, a large majority will relearn some of their motor skills by performing repetitive tasks in therapy [3]. A key factor in improving rehabilitation is progress measurement. Progress measurement involves collecting the data on the relearning rate of the affected joint and the patient's recovery in general. Furthermore, 45% of post-stroke patients return home and still need ongoing therapy to recover their motor skills [4]. Therefore, only patients who can afford private therapists who visit to take measurements have chances of a full recovery. Even with a private therapist, there is a chance that their visits might not coincide with rare occurrences that are important to the patient's progress measurement [5].

Therefore, an approach is needed that enables the collection of data from the the patient's hand without the need to schedule a therapist's appointment. There are two major methods in measuring the flexion of finger joints and they are camera-based and data glove approaches. Camera-based approach involves the use of a camera and markers in which images acquired are processed to calculate the flexion at the joints [6], [7]. Although the accuracy of this approach has been improved by the use of more novel and complex image processing techniques, they are not commercially feasible in remote monitoring due to privacy concerns as these cameras can be vulnerable to attacks and could be used to record the private lives of the patients. Furthermore, the use of stationary cameras deprives the patient of free movement as they have to be stationary for the camera to accurately capture the fingers motion. Multiple cameras such as in [8] could alleviate this problem but this increases cost and may be higher than the cost of multiple therapist home visits.

In contrast, data gloves provide a cheaper and more efficient alternative as the patient can wear it while performing their daily activities. However, the conventional design of data gloves prevent their large scale adoption in the rehabilitation industry. Particularly, the conventional design comprises of an external attachment that adheres the sensors to the support structure. The support structure is usually a textile glove that places the sensors at the phalangeal joints. This design causes the data glove to be bulky and produce inconsistent results progressively with the degradation of the attachment. Table I illustrates a summarised review of different data gloves, highlighting their sensors and the method of attachment. Fabric padding is the most common method of attachment in data gloves. It involves placing strain sensors such as fibre-optic and flex sensors in between multiple layers of fabric in a textile glove. Popular commercial data gloves such as Cyberglove and 5DT 5 Ultra have utilised this method [9], [10], [11], [12]. However, this leads to at least three layers of sensor and support structure which causes a bulky data glove and might impede the progress of patients in sensitive applications.

Ink printing is a great lightweight alternative to the fabric padding method as it involves printing conductive ink on a textile glove at phalanx joint locations. This ensures that the glove is not as bulky as the number of layers are limited to one in most places and two in the phalanx joints [13][24]. However, conductive inks are vulnerable to environmental degradation which will lead to inconsistent results when the data gloves are not used in the optimum environmental conditions. Other chemical methods of attachment such as silicon rubber curing and cyanoacrilic glue are also degradable and will eventually lead to distorted results.

In contrast, weft knit sensors present a unique potential in the design of wearable devices as the sensors and the support structure can be created in a single knitting process. Particularly, knee sleeves and respiration belts have been

[1]Institute of Robotics, Autonomous Systems and Sensing; University of Leeds. UK. Syed Ali Raza Zaidi is the corresponding author - S.A.Zaidi@leeds.ac.uk.

[2]School of Architecture, Planning & Landscape, Newcastle University, Newcastle, UK.

[3]Department of Electrical Engineering. Faculty of Engineering. The Hashemite University. P.O. Box 330127, Zarqa 13133, Jordan.

[4]School of Engineering and Computer Science, University of Hull. UK

TABLE I
A COMPARISON OF DATA GLOVES.

Type of Sensor	Attachment method	Reference
Conductive elastomer composites	Ink printing	[13]
Fibre optical sensors (5DT 5 Ultra)	Fabric padding	[9], [10], [12]
Hall effect sensors	Fabric padding	[14]
Piezo-resistive sensors (Cyberglove)	Fabric padding	[11]
Magnetic sensing coils	Electrical wires	[15]
Flex sensors	Fabric padding	[16], [17], [18], [19], [20]
Accelerometers (KHU-1)	Hook-and-loop fasteners	[21]
Flex sensors	Cyanoacrilic glue	[22]
Bend sensors and IMUs	Fabric padding	[23]
Conductive polymer (PEDOT:PSS) ink	Ink jet printing	[24]
IMUs and force sensors	Cable ties	[25]
IMUs	Hook-and-loop fasteners	[26], [27]
Soft sensor	Silicon rubber curing	[28]
IMUs	Textile cables	[29]
Metalized fabric conductors	Sewing and fabric padding	[30]
Bend sensors (Shadow glove)	Plastic sheath padding	[31]
Semi-Conducting scotch tape	Fabric padding	[32]

developed using weft knit sensors [33], [34], [35]. However, there has been no data glove created with weft knit sensors.

Therefore, this paper presents a weft knit smart data glove capable of measuring the finger flexion at the interphalangeal joints is proposed. Furthermore, this glove utilises Whole-Garment technology to fabricate the sensors and the support structure in a single manufacturing process thus eliminating the need for an external attachment. This ensures that the glove is unobtrusive, lightweight and accurate. Additionally, the glove is commercially feasible because custom-sized data gloves can be manufactured easily as we depart from a one-size-fits-all philosophy.

In addition, a novel loop configuration comprising of an elastomeric yarn and a conductive yarn is knitted in a plain structure to create the sensor. Moreover, the electromechanical behaviour of this sensor is modelled using Postle's geometrical model [36] and validated experimentally. The advantage of using Postle's model is that it enables the modelling of the length of the loop legs and head based on the loop's interlocking and loop angles. Finally, the weft knit data glove is validated in terms of its consistency and the performance of some classical machine learning algorithms on the application of the glove in a classification scenario is evaluated.

B. Related Work

Weft knitting is one of the most popular knitting techniques and it involves interlocking loops of yarn in a horizontal direction such that the feet of the loop legs lock with the head of the previous knitting cycle's loops [37]. Therefore, when conductive yarn is weft knitted, contact resistances occur because of the interlocking of conductive loops. The contact resistance is dependent on the contact pressure between the interlocked loops which varies based on the load applied on the sensor [38], [39], [40].

Consequently, the weft knit sensor is classified as a piezoresistive sensor due to the changes in the resistance of the sensor caused by the applied load. The conductive yarn could be a yarn coated with conductive ink or a multifilament yarn comprising of stainless steel fibres. Multifilament conductive yarns are preferable to silver-coated yarns in the creation of wearable sensors because they are more environmentally stable [41]. Furthermore, the behaviour of the sensor is dependent on the sensor's knit structure and its knitting parameters.

The strain sensing properties of weft knit fabric knitted with conductive yarn was investigated in [42]. The sensor was knitted in a plain knit structure with a stainless steel multifilament conductive yarn and tested experimentally to observe the sensor's piezo-resistivity. It was observed that the resistance of the sensor reduced exponentially as the load applied increased. This occurred because the contact resistance formed by the contact between the interlocked loops of conductive yarns varied due to the change in contact pressure caused by the load applied.

Furthermore, the effect of mechanical preconditioning was investigated in [43]. Different sensors were knitted in a plain knit structure but with different loop configurations and were experimentally tested. Subsequently, it was observed that mechanical preconditioning caused the resistance of the sensors to reduce till it reached a stabilised value.

In addition, Atalay et al. [44], [45] investigated the effect of the conductive yarn's input tension and linear density on the sensor's piezo-resistivity. In contrast, the sensor was knitted in an interlock structure. It was observed that the electrical resistance of the sensor increased when the input tension or the linear density was decreased. This effect materialised because the input tension and the linear density affected the contact pressure between the intermeshed loops.

Despite the breakthroughs in these investigations, there have been few studies illustrating the application of weft knit sensors in motion capture. Particularly, a respiration monitoring belt was developed using an interlock knit strain sensor [35]. The belt measured the respiration rate from the expansion and contraction of the abdominal area. Moreover, the sensor's electromechanical model was derived from the Peirce's [46] geometrical model. This model derived the lengths of the loop head and legs from the diameter of the yarn used. Additionally, the sensor was knitted with conductive yarn made by coating non-conductive yarn with silver.

Conventionally, the creation of knitted garments followed the design methodology of current data gloves. It involved

knitting the different parts of the garment separately and then attaching them by sewing. However, the introduction of WholeGarment technology has facilitated the fabrication of entire knitted garments in a single process. This is relevant in the creation of textile sensors because it enables the creation of both the sensors and the non-conductive support structure in the same fabrication process. Additionally, in applications which might require a complex design of the sensor such as for progress measurement in the knee or ankle, it enables the creation of the sensor in a single process. This is advantageous because sewing different parts of the sensor together will impact the extensibility and the piezoresistive behaviour of the sensor.

C. Contributions

The main contributions of this paper are as follows:

1) We propose a novel electromechanical model of a weft knit sensor based on the loop and interlocking angles in the conductive loops. In addition, we devise an algorithm that simplifies the computation of the contact resistance between each intermesh of conductive loops from the equivalent resistance of the sensor. Moreover, we validate the accuracy of the model experimentally in a tensile test.
2) We design a novel textile data glove comprising of weft knit sensors with no external attachment between the sensors and the support structure. The configuration of the sensors are novel and we observe their repeatability in a flexion-extension experiment.
3) We investigate the effect of drift in the sensor's output on the performance of machine learning algorithms in a classification scenario. Notably, it is the first time machine learning algorithms have been utilised in classifying data from a weft knit sensor.

II. Weft Knit Sensor

The weft knit sensor was designed with a novel combination of conductive and elastomeric yarn knitted in a plain knit structure. The design is illustrated in Fig. 1. Unlike [42] where the sensor was knitted with only conductive yarn, we integrated an elastomeric yarn to create a more elastic sensor. Particularly, we achieve this by knitting 50% of the courses with elastomeric yarn in a pattern where a course of conductive yarn courses is succeeded by a course of elastomeric yarn loops and is repeated till the last course of the sensor. In addition, a plain knit structure was selected ahead of an interlock structure because interlock knitted fabrics are less extensible than plain knitted fabrics.

A. Electromechanical Model

The conductive yarn used in fabricating the sensor is a multifilament yarn comprising of 80% polyester and 20% stainless steel. Due to the metallic properties of the conductive yarn, its length resistances of the loop head and legs were modelled as R_h and R_l while the contact resistances between interlocking conductive yarn loops were modelled as R_c. The model also follows the basic assumption that the geometry of each loop is constant across the sensor.

Due to the knitting action of the cam box in a knitting machine, when two yarns are used interchangeably across different courses, there is a crossover at the edge of the fabric between the previous and the current course knitted by the same yarn. In our sensor, the crossover between the conductive courses is modelled as R_{co}. The combination of the resistances in a conductive course and its respective crossover is termed as a conductive section. The equivalent resistance of each n conductive section is modelled as $R_{s(n)}$. Therefore, the circuit of the sensor represented in Fig. 2 represents a series network of conductive sections and the number of conductive sections is equal to the number of conductive courses in the sensor.

$V_{s(n)}$ represents the voltage across each conductive section. Due to the aforementioned modelling assumption stating that the geometry of each conductive loop is constant across the sensor, the equivalent resistances of the conductive sections are equal. Thus, the voltage across each conductive section, $V_{s(n)}$ is calculated as:

$$V_{s(n)} = \frac{V}{n}, \tag{1}$$

where V is the voltage across the sensor. Let I_1 - I_Z represent the hypothetical currents flowing in the meshes of the circuit (as shown in Fig. 2) and are solved using Kirchoff voltage law and Ohm's law as:

$$\mathbf{i} = \mathbf{R}^{-1}\mathbf{v}, \tag{2}$$

where in a sensor with 72 courses (36 conductive courses) and 36 wales (i.e. Z=37),

$$\mathbf{i} = [I_1, I_2, \ldots, I_{36}, I_{37}]^T, \tag{3}$$

$$\mathbf{v} = [V_{s(n)}, \underbrace{0, \ldots, 0, 0}_{36 zeros}]^T, \tag{4}$$

The equivalent resistance of each conductive section is calculated as:

$$R_{s(n)} = \frac{V_{s(n)}}{I_1}. \tag{6}$$

B. Determination of Length Resistances

The length resistances are derived from the Postle's geometrical model of a weft knit loop [36]. This model determines the length of the loop legs and head from the loop and interlocking angles of the loop. The loop angle, α, is the angle between the loop's tangent and the vertical at the centre locus of the loop while the interlocking angle, β, is the angle at the interlocking locus between the loop's tangent and the vertical.

By considering the loop leg as a bent beam, its length was derived as:

$$L_l = \frac{p}{\sqrt{2(\sin(\alpha) + \sin(\beta))}} f(k, \gamma), \tag{7}$$

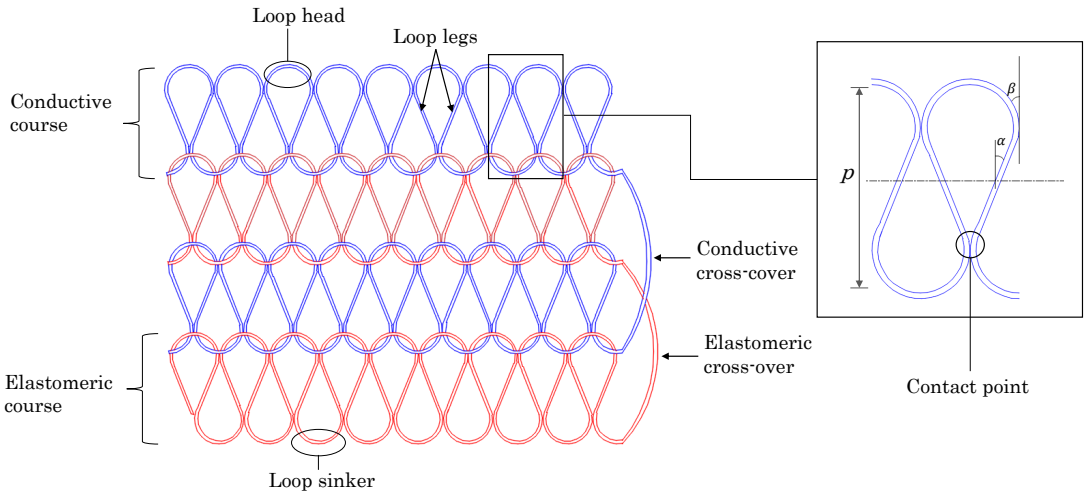

Fig. 1. Design of the Weft Knit sensor. α is the loop angle, β is the interlocking angle and a course represents a horizontal row of knitted loops.

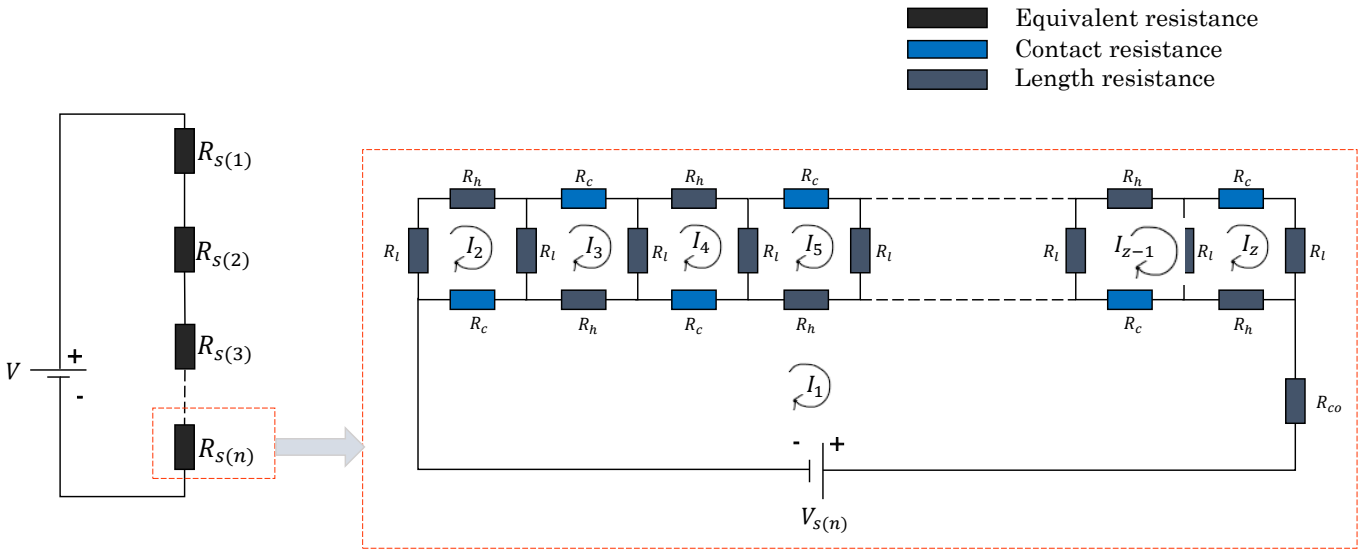

Fig. 2. Circuit model of the weft knit sensor. $(Z-1)$ is the number of wales in the sensor.

where p is the course spacing. $f(k,\gamma)$ is the difference between the complete and incomplete integrals and can be calculated as:

$$f(k,\gamma) = \int_0^{\frac{\pi}{2}} \frac{d\gamma}{\sqrt{1-k^2\sin^2(\gamma)}} - \int_0^{\gamma} \frac{d\gamma}{\sqrt{1-k^2\sin^2(\gamma)}}, \tag{8}$$

and parameters k and γ are calculated as:

$$k = \sin\left(\frac{\pi}{4} + \frac{\alpha}{2}\right), \tag{9}$$

$$\gamma = \sin^{-1}\left(\frac{1}{k\sqrt{2}}\left(\cos\left(\frac{\beta}{2}\right) - \sin\left(\frac{\beta}{2}\right)\right)\right). \tag{10}$$

The length of the loop head was considered to be the sum of two equal segments of a circle and is derived as:

$$L_h = \frac{p(\frac{\pi}{2}-\beta)}{2(\sin(\alpha)+\sin(\beta))}. \tag{11}$$

The resistances of the held loop's legs and head are then calculated as:

$$R_l = \frac{\rho L_l}{A_r}, \tag{12}$$

$$R_h = \frac{\rho L_h}{A_r}. \tag{13}$$

where A_r is the cross-sectional area of the conductive yarn. The length of the crossover was empirically observed to be twice the course spacing, p. Therefore, the resistance of the conductive crossover is calculated as:

$$R_{co} = \frac{2p\cdot\rho}{A_r}. \tag{14}$$

C. Determination of Contact Resistance

Contact resistance only occurs when there is contact between two conductors. Particularly, it occurs at the contact

$$\mathbf{R} = \begin{bmatrix} 18(R_c + R_h) + R_{co} & -R_c & -R_h & \dots & -R_h \\ -R_c & R_c + R_h + 2R_l & -R_l & \dots & 0 \\ -R_h & -R_l & R_c + R_h + 2R_l & \dots & 0 \\ -R_c & 0 & -R_l & \dots & 0 \\ \dots & \dots & \dots & \dots & \dots \\ -R_c & 0 & 0 & \dots & R_c + R_h + 2R_l \end{bmatrix}. \quad (5)$$

between the conductive loop legs as illustrated in the enlarged frame in Fig. 1. According to Holm's contact theory, the contact resistance can be calculated as:

$$R_c = \frac{\rho}{2}\sqrt{\frac{\pi H}{nP_r}}, \quad (15)$$

where, R_c is the contact resistance, ρ is the electrical resistivity, H is the hardness of the material used, n is the number of contact points and P_r is the contact pressure between the conducting materials.

Typically, the material hardness and the electrical resistivity are constant based on the properties of conductive yarn used, while the number of contact points is subject to the sensor's design. Therefore, the changes to the contact resistance is dependent on changes to the contact pressure between the loops.

However, simulating or predicting the contact pressure between the interlocking loops has proven cumbersome due to the geometrical complexity of a weft knit sensor. Therefore, alternative methods such as obtaining the contact resistance empirically from the contact force have been proposed [35]. However, Zhang et al. [42] suggested from experimental observations that the relationship between the contact and equivalent resistances can be depicted as:

$$R_{eq} = R_c D, \quad (16)$$

where D is a variable coefficient based on the sensor design.

By using a control algorithm illustrated in algorithm 1, we determine the contact resistance from the equivalent resistance. The algorithm is initialised with any positive value as D. Subsequently, the algorithm employs a control feedback by inputting the calculated contact resistance into the modelled circuit. The output equivalent resistance termed as $Rsim$ is then used to determine the new coefficient, D. The optimised contact resistance is produced when the difference between the previous simulated equivalent resistance and its current value is less than 3% of the current value. This threshold was chosen empirically as no significant change in accuracy of the model was detected below the threshold.

Algorithm 1 Contact Resistance Solution

Initialise:
$R_{sim} \leftarrow 0$
$D \leftarrow 0 < D < \inf$
Loop:
$R_c = R_{exp}/D$
Input R_c into modelled circuit to determine R_{sim}
if $|R_{sim(n)} - R_{sim(n-1)}| > (0.03 \cdot R_{sim(n)})$ **then**
    $D = R_{sim}/R_c$
    goto *Loop*
else
    Return R_c
end if
▷ R_{sim} and R_{exp} are the simulated and experimental equivalent resistances respectively.

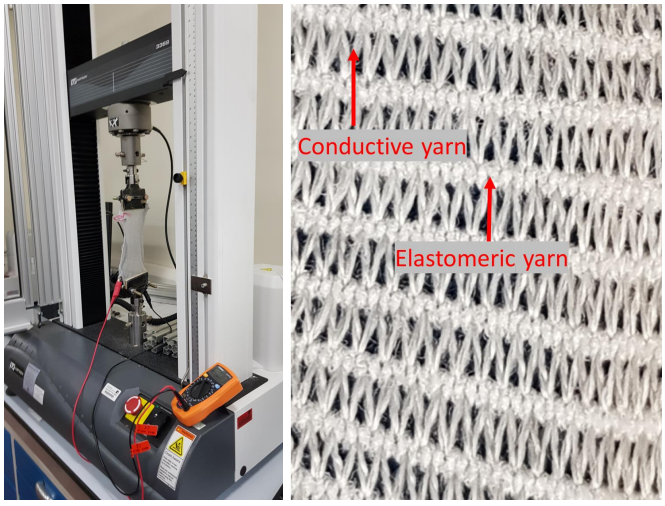

(a) (b)

Fig. 3. (a) Experimental setup with Instron 3369 and Multimeter. (b) Image of sensor's loop configuration.

D. Model Validation

This model was verified by fabricating sensors with the aforementioned sensor design and the knitting parameters enumerated in Table II. Subsequently, the sensors were dry relaxed for 48 hours to remove any excess strain between the loops as a result of the knitting process. The sensors were then put through a tensile test in an Instron3369 tensile machine where it was extended till 35% extension while its resistance was measured with a digital multimeter. The loop configuration of the sensor and the experimental setup are shown in Fig. 3. Furthermore, a simulation of the model was also performed using Matlab and LTspice with the same numerical parameters.

III. Data Glove

The weft knit data glove was designed using Shima Seiki's sds one apex3 apparel CAD software such that the weft knit sensors were located at the distal and proximal interphalangeal joints while the rest of the glove was knitted with an elastomeric yarn. Particularly, the sensors were knitted to wrap around the joints to maximise its sensitivity. An elastomeric

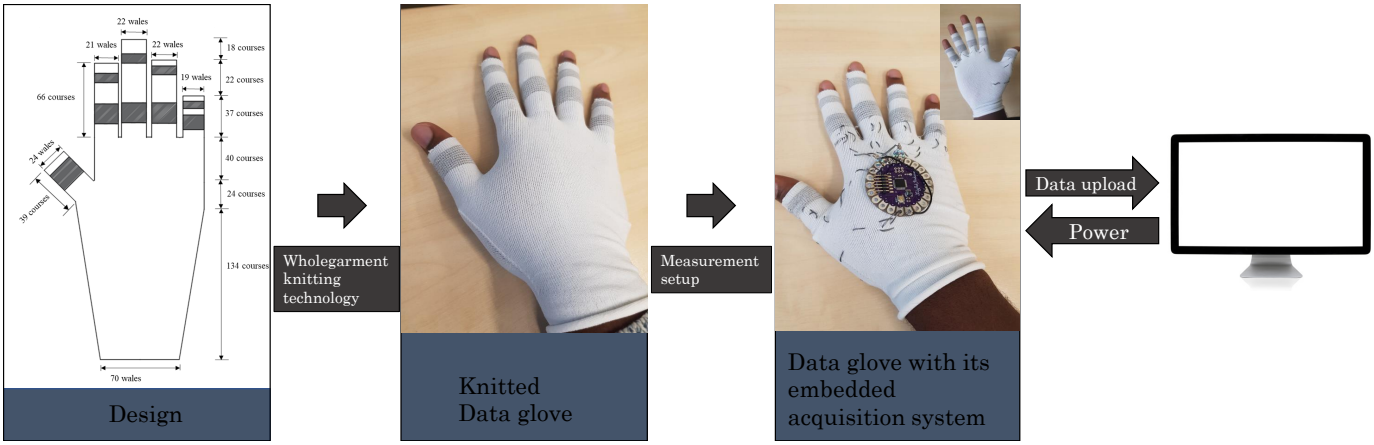

Fig. 4. Block diagram illustrating the design and implementation of the weft knit Data glove.

TABLE II
NUMERICAL PARAMETERS FOR SIMULATION AND EXPERIMENTAL VALIDATION

Parameters	Values
Number of conductive courses	36
Number of elastomeric courses	36
Number of wales	36
α	$24.75°$
β	$10.85°$
Course spacing	3mm
Yarn diameter	0.4mm
Resistivity	300(ohm·mm)

yarn was selected for the rest of the glove because it provides a tight and flexible fit that is optimal for sensing applications while also providing a comfortable experience for the user. WholeGarment technology enabled the knitting of all sensors and the support structure of the glove in a single manufacturing process without any external attachment. The glove design and the fabricated glove are illustrated in Fig. 4. The glove was knitted with Shima Seiki Mach2s which is equipped with WholeGarment technology. Furthermore, the dimensions used in knitting the glove were selected based on the main author's hand size. This illustrates its commercial feasibility as several data gloves can be fabricated based on sizes similar to the creation of conventional fabrics.

A. Data Acquisition

A data acquisition system is embedded in the glove to transmit data to a computer. Particularly, it consists of a microprocessor and a set of resistors that form a voltage divider circuit with the ADCs (analog-digital converter) of the microprocessor. The microprocessor used was an Arduino lilypad and it was selected because of its 6 analog inputs which can be connected to the sensors via sewing. However, due to the limited number of analog inputs in the microprocessor, only the sensors at the PIP (proximal interphalangeal) joints were connected to the microprocessor. In our subsequent work, a custom-made microprocessor with 9 analog inputs and wireless capabilities will be embedded on the glove to retrieve data from all sensors and remotely transmit it to a cloud platform.

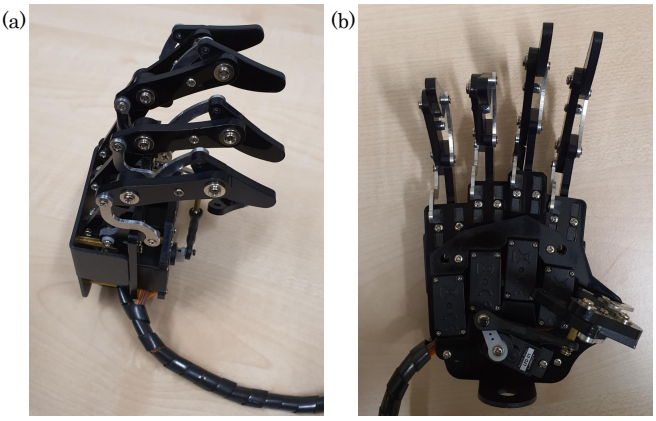

Fig. 5. Robotic hand used for glove evaluation. (a) Side view (b) Front view illustrating its motors.

Furthermore, the sensors at the PIP joints were connected to the analog inputs of the microprocessor by sewing conductive thread in front of the glove while the sensors were also connected to the negative pin of the microprocessor at the back of the glove to prevent a short circuit between the positive and negative threads. These analog inputs have individual ADCs that convert analog voltages between 0 and 3.3volts to digital values between 0 and 1023. This allows the microprocessor to read the data of all fingers in parallel. The microprocessor was programmed to transmit data from the sensor at a frequency of 100 Hertz. However, the analog output of weft knit sensors is electrical resistance, therefore a voltage divider circuit is required to convert the sensor's resistance to voltage. The sensor voltage is obtained as:

$$V_{sensor} = V_{input} \cdot \frac{R_{sensor}}{R_{fixed} + R_{sensor}}, \tag{17}$$

where V_{sensor} is the calculated sensor's voltage, V_{input} is the input voltage, R_{fixed} is a fixed resistor value and R_{sensor} is the variable resistance of the weft knit sensor. Furthermore, the computer also provides power to the microprocessor although a coin-cell battery can be embedded in the glove to enable it store data for upload at a later date.

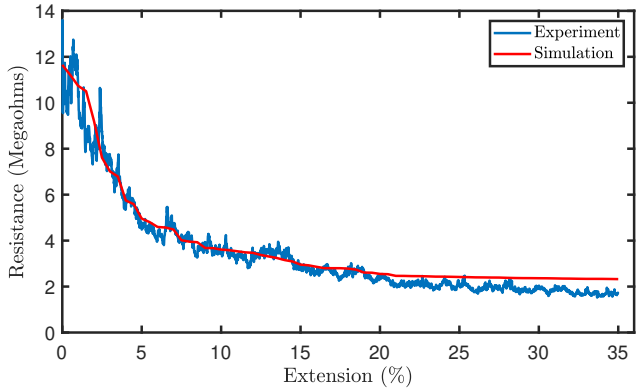

Fig. 6. Experimental and simulation results of strain test.

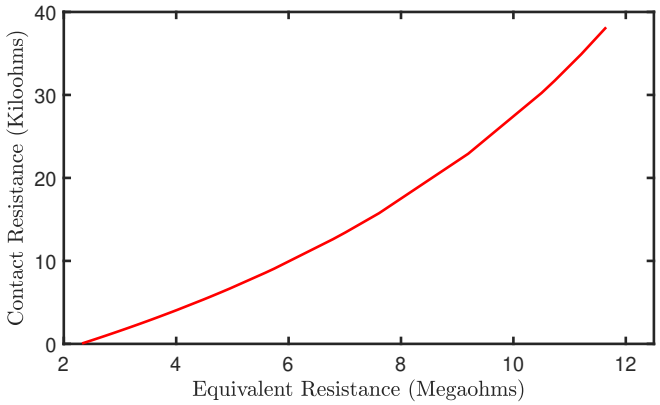

Fig. 7. Relationship between the contact resistance between the conductive loops and the equivalent resistance of the sensor.

B. Glove Evaluation

The robotic hand shown in Fig. 5 was applied as an emulation tool in evaluating the glove's sensor. Its joint angle was set accurately without constraints such as fatigue and stability that may plague human participants when instructed to maintain a posture for a considerable period. The robot was obtained commercially and consists of stepper motors that control the joints at each finger. All evaluations were performed with the proximal interphalangeal joint of the middle finger of the robot.

1) Flexion and Extension: The first experiment consists of the opening (extension) and closing (flexion) of the hand. This test simulates one of the prominent hand motions and depicts the repeatability of the sensor. The robot was programmed to perform this at a frequency of one oscillation every 18 seconds.

2) Drift: Weft knit sensors are known to observe phenomena such as hysteresis and drift that negatively impact the sensor's output [44]. Drift occurs when the sensor's output stray away from the original measurement when the extension of the sensor is constant.

A second experiment was performed to visualise the drift in the sensor and illustrate the use of machine learning in reducing the impact of this phenomenon in a classification scenario. In this scenario, the sensor's output was recorded when the joint was held at $0°$, $15°$, $30°$, $45°$, $60°$ and $75°$ for 90 seconds. The first 5 seconds and the last 5 seconds were eliminated to remove the noise caused by the impact of switching to the next angle. Subsequently, classical machine learning algorithms such as Support vector machines (SVM), Logistic Regression and Gaussian naïve Bayes were used to classify the sensor's output.

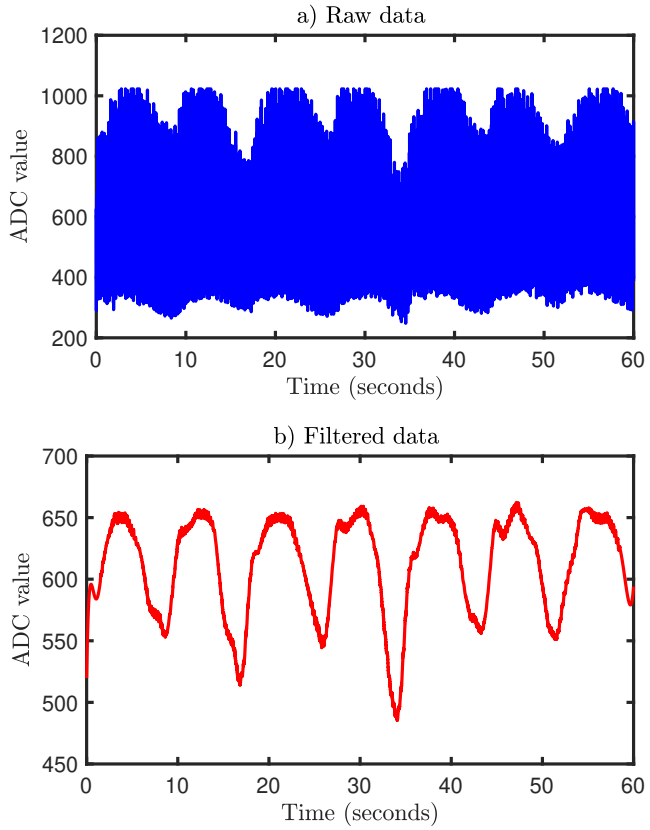

Fig. 8. Flexion and extension experimental result.

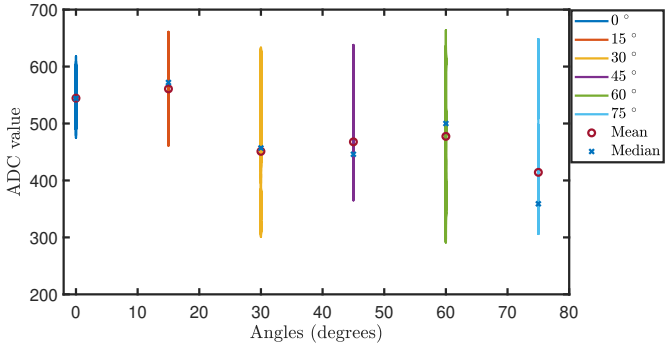

Fig. 9. Data plot of drift experimental result. Mean and median are shown to illustrate skew of data.

IV. Results and Discussion

A. Model Validation

The average experimental and simulation results of the strain test are illustrated in Fig. 6. The sensor exhibits an exponential relationship between its resistance and extension. The piezoresistivity plot of the sensor can be divided into three

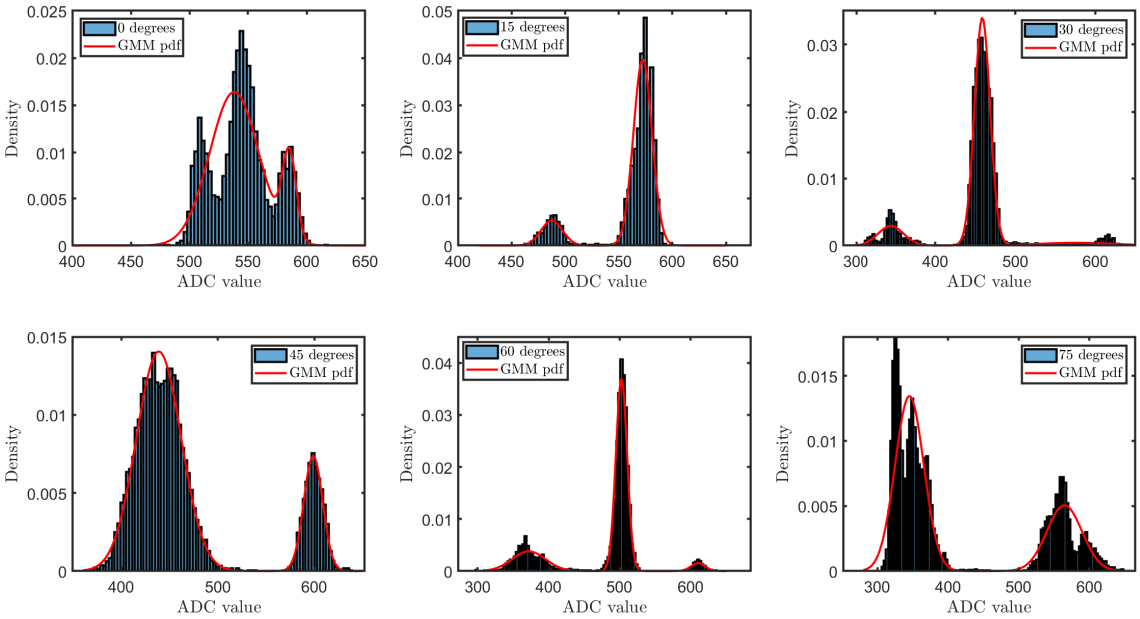

Fig. 10. Histogram plots and respective mixed gaussian distribution fits of the sensor's output at (a) 0° (b) 15° (c) 30° (d) 45° (e) 60° (f) 75°

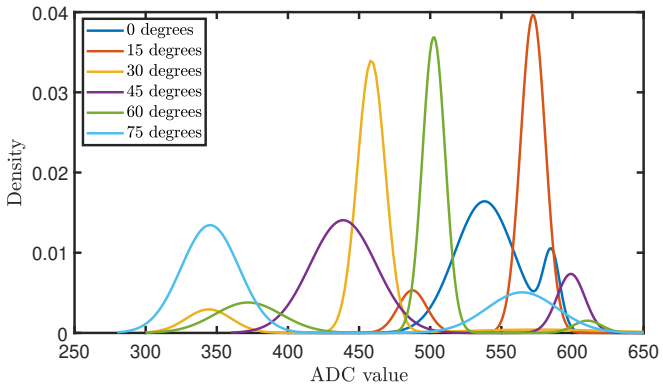

Fig. 11. Mixed gaussian distribution fits of the sensor's output at various angles.

phases. In the first two phases, the sensor resistance decreases linearly as the sensor is extended but the slope of decrease varies between the two phases. In the third phase, the sensor's resistance is relatively constant. This occurs because at this level of extension, the contact resistances between certain conductive loops in the sensor are negligible. The first linear phase occurs between 0% and 6% extension, the second linear phase occurs between 6% and 25%, and the third phase occurs after 25% extension. Our simulation results largely agree with the experimental results. Particularly, the average percentage error between the simulation and experimental for the entire range of extension was 11.47%. However, the error was lower when excluding the third phase. The average percentage error in the linear phases was 7.33% while the average percentage error in the third phase was 21.66%. The increase in the error in the third phase ensued because of the difficulty in simulating the specific loops whose contact resistances are negligible when the sensor is extended beyond 25%. Particularly, our simulation assumes uniform behaviour across all knit loops in the sensor but in reality, this is not the case especially as the sensor approaches its breaking point.

In addition, we illustrate the relationship between the derived contact resistance and the simulated equivalent resistance at each level of strain in Fig. 7. We observed that the change in contact resistance between the conductive loops is directly proportional to the change in the equivalent resistance of the sensor. Moreover, the R^2 value of its linear fit was calculated to be 0.9742, thereby showing a high linearity of the relationship between the contact resistance and the equivalent resistance. This is important because it can simplify future simulations of the electromechanical behaviour of weft knit sensors. Furthermore, this relationship explains the contact between the loops as the sensor is stretched. From equation 15, we observe that the contact pressure is inversely proportional to the contact resistance. Therefore, since the equivalent resistance is directly proportional to the contact resistance, we assume that the equivalent resistance is inversely proportional to the contact pressure. Furthermore, by observing the relationship between the equivalent resistance and the extension of the sensor in Fig 6, we derive that the contact pressure between the conductive loops increases exponentially as the sensor is extended.

B. Glove Evaluation

1) Flexion and Extension: Fig. 8 shows the result of the flexion and extension at the robot's joint. Due to the high sampling rate, the sensor's output was very noisy. Therefore, a Savitzky-Golay filter (polynomial order of 5 and window

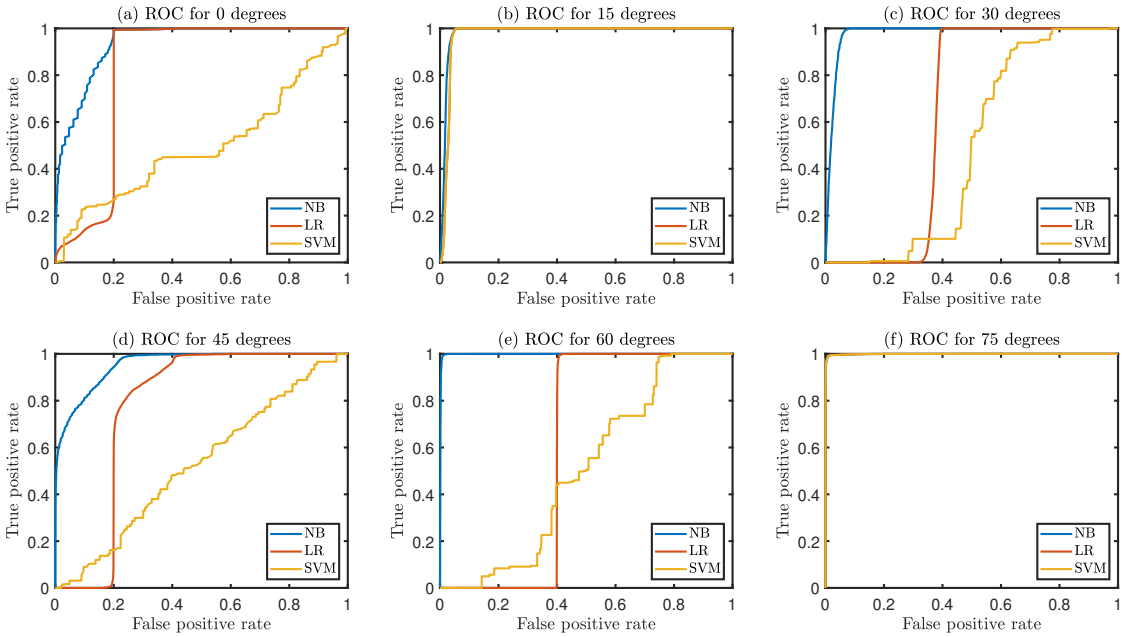

Fig. 12. Receiver operating curve for the classifiers at the different angles. NB, LR and SVM represent Gaussian naïve Bayes, Logistic regression and Support vector machine classifiers respectively.

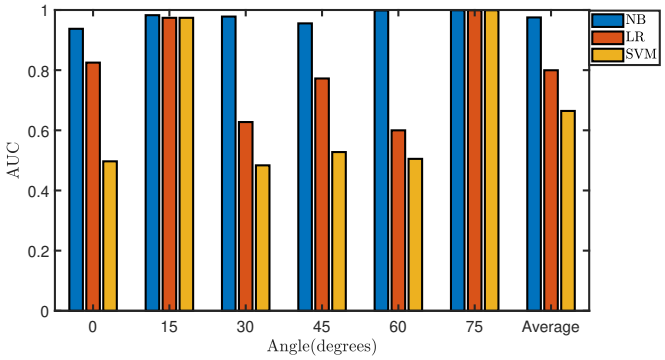

Fig. 13. Area under the ROC for the different classifiers at the various angles.

length of 301) was applied on the output. The filter removes most of the noise that was present in the raw signal and illustrates the repeatability of the sinusoidal oscillations in the sensor's output. However, there are still minor distortions in the filtered signal. These distortions represent the hysteresis and drift common in weft knit strain sensors.

2) Drift: The sensor's output at each angle threshold in the drifting experiment is shown in Fig. 9. This figure provides a preliminary visualisation of the experiment's results. The mean and median values illustrate the skew of the data. We observed that the output of the sensor reduced as the angle increased for most of the experiment. However, some angles opposed this observation. This was expected as prior experimental results from the tensile test had shown instability and non-linearity in the sensor's output. In addition, we hypothesise that the high sampling rate may have increased the noise in the sensory data.

A detailed visualisation of the data is illustrated in Fig. 10 with an histogram plot and its probability distribution fit. As illustrated in the histogram plots, the sensor's output fluctuates despite the fixed angle of the robot's joint. However, we observe that the most of the data were within a limited range during these fluctuations. Particularly, we observe that the data at each angle were mostly distributed into two classes. Therefore, we implemented a mixed Gaussian distribution (MGD) using expected maximisation (EM) algorithm [47] to provide an accurate fit of the data. We also limited the number of classes to two based on our empirical observations to prevent overfitting. From the MGD fits, we observed that one class was significantly smaller than the other class in terms of the density. We hypothesise that the smaller class is noise and the bigger class is the real signal. However, we did not eliminate the noise to prevent biasing the results of the classifiers.

Furthermore, we plot the MGD fits of all angles in Fig. 11. This depicts a comprehensive view of the effect of drift on the sensor's output. We observed that drift causes the distribution fits of the angles to overlap each other. In particular, the presence of drift in the sensor's output may adversely affect the performance of linear classifiers.

Subsequently, we evaluate the performance of three classifiers in accurately classifying the sensor's data. These classifiers are Linear SVM, Logistic Regression and Gaussian naïve Bayes algorithms [48], [49]. Particularly, each classifier is evaluated on its performance in classifying the data of a specific angle from all other angles. The data consisted of 4000 samples for each angle (24,000 samples in total) with each sample representing 20 milliseconds thereby reflecting real-time measurement. The temporal order was kept unchanged

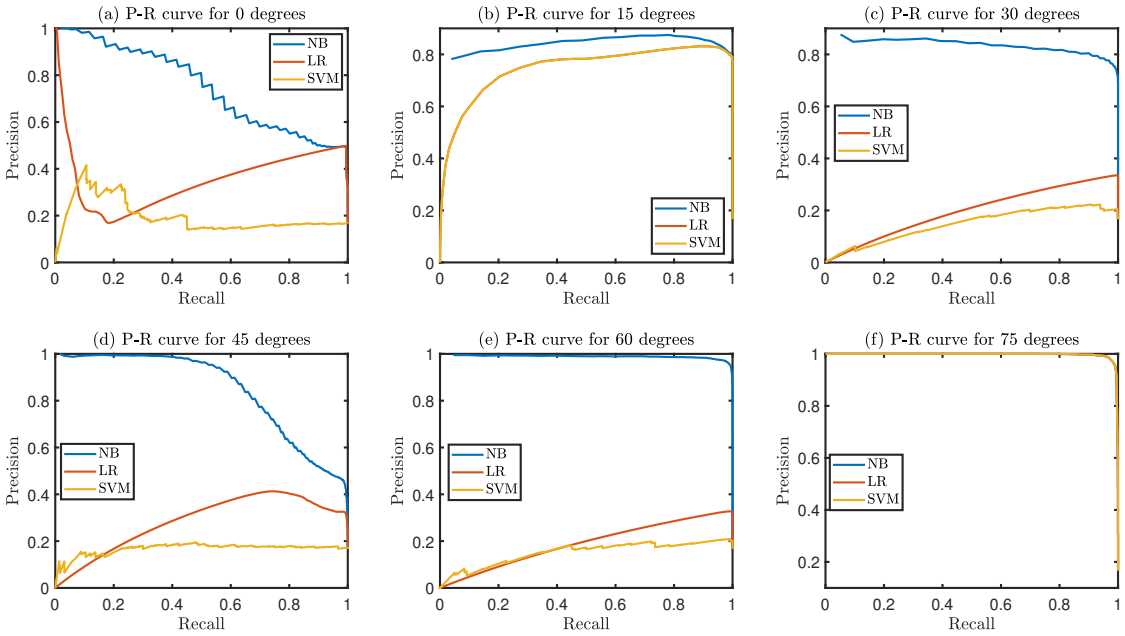

Fig. 14. Precision-Recall curve for the classifiers at the different angles.

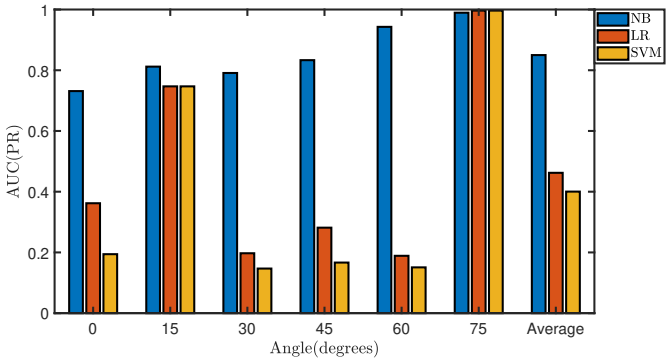

Fig. 15. Area under the Precision-Recall curve for the different classifiers at the various angles.

and no additional pre-processing techniques were applied on the data as it would be impractical due to the novelty of weft knit strain sensors. In addition, it was important that the classifiers were applied on the raw sensory data to accurately investigate the effect of drift. The classifiers were trained and validated using 10-fold cross-validation to prevent overfitting.

The performance metric for evaluating the classifiers is the area under the receiver operating curve. Firstly, a confusion matrix comprising of the true positive rate (TPR) and the false positive rate (FPR) of the classifier is computed. The TPR is the proportion of correctly identified data values while the FPR is the proportion of incorrectly identified data values. The TPR and FPR for each classifier is plotted as a receiver operating curve (ROC). The area under the ROC (AUC) is then calculated using the trapezoidal rule.

The classification results are shown in Fig. 12 and Fig. 13. We observed that Gaussian naïve Bayes classifier performed better than other classifiers with an average AUC of 0.9753 while Logistic regression and SVM had an average AUC of 0.7997 and 0.6644 respectively. Logistic regression under-performed because as observed in the visualisation of the data, the overlap of data from different angles complicate the linear classification of the data. Moreover, this also explains why SVM under-performed because of the difficulty of its linear kernel in classifying the data. It is likely that if a non-linear kernel such as the Gaussian kernel is implemented, it would improve its performance. Consequently, the Gaussian naïve Bayes classifier performed adequately because of its non-linear kernel.

In addition, the Precision-Recall curve and the area under the curve are illustrated in Fig. 14 and Fig. 15. The results further reinforce the superiority of non-linear algorithms over linear algorithms in classifying the data of weft knit strain sensors. In particular, the average area under the precision-recall curve was 0.85, 0.46 and 0.4 for the Gaussian naïve Bayes, Logistic regression and Linear SVM respectively. These results show that non-linear classifiers can accurately classify sensory data from weft knit strain sensors in spite of the noise, hysteresis and drift. In contrast, linear classifiers may struggle to accurately classify the sensory data of weft knit strain sensors.

V. Conclusion

In this paper, we have proposed a wholly textile data glove capable of measuring the joint angles of the interphalangeal joints. We achieved this by creating its novel weft knit sensors and its textile support structure in a single fabrication process. Additionally, we presented the electromechanical model of its sensors and verified it experimentally. Moreover, we evaluate

the repeatability of the glove in a flexion and extension experiment. The results show that when a filter is applied to remove the noise, the glove performs excellently. Furthermore, we evaluate three machine learning algorithms in classifying the output of the data. We observe that the drift in the sensor limits the performance of linear classification algorithms. However, the performance of naïve Bayes classifier illustrates that a non-linear classifier can perform excellently in classifying the glove's output.

Future work will investigate the performance of deep learning algorithms in a real-world classification scenario such as grasp or gesture recognition. The glove will also be improved by creating a wireless version with an embedded power source to make it a portable system that can be used without any movement constraints.

REFERENCES

[1] N. J. Seo, W. Z. Rymer, and D. G. Kamper, "Delays in grip initiation and termination in persons with stroke: effects of arm support and active muscle stretch exercise," *Journal of neurophysiology*, vol. 101, no. 6, pp. 3108–3115, 2009.

[2] M. H. Schieber, C. Lang, K. Reilly, P. McNulty, and A. Sirigu, "Selective activation of human finger muscles after stroke or amputation," in *Progress in Motor Control*. Springer, 2009, pp. 559–575.

[3] C.-y. Park, J.-h. Bae, and I. Moon, "Development of wireless data glove for unrestricted upper-extremity rehabilitation system," in *ICCAS-SICE, 2009*. IEEE, 2009, pp. 790–793.

[4] R. V. Aroca, R. S. Inoue, L. M. Pedro, G. A. Caurin, and D. V. Magalhaes, "Towards a battery-free wireless smart glove for rehabilitation applications based on rfid," in *RFID, 2015 IEEE Brasil*. IEEE, 2015, pp. 1–5.

[5] C. OQuigley, M. Sabourin, S. Coyle, J. Connolly, J. Condall, K. Curran, B. Corcoran, and D. Diamond, "Characteristics of a piezo-resistive fabric stretch sensor glove for home-monitoring of rheumatoid arthritis," in *Wearable and Implantable Body Sensor Networks Workshops (BSN Workshops), 2014 11th International Conference on*. IEEE, 2014, pp. 23–26.

[6] G. S. Rash, P. P. Belliappa, M. P. Wachowiak, N. N. Somia, and A. Gupta, "A demonstration of the validity of a 3-d video motion analysis method for measuring finger flexion and extension," *Journal of Biomechanics*, vol. 32, no. 12, pp. 1337–1341, 1999.

[7] R. Y. Wang and J. Popović, "Real-time hand-tracking with a color glove," *ACM transactions on graphics (TOG)*, vol. 28, no. 3, p. 63, 2009.

[8] P. Braido and X. Zhang, "Quantitative analysis of finger motion coordination in hand manipulative and gestic acts," *Human Movement Science*, vol. 22, no. 6, pp. 661–678, 2004.

[9] O. Luzanin and M. Plancak, "Hand gesture recognition using low-budget data glove and cluster-trained probabilistic neural network," *Assembly Automation*, vol. 34, no. 1, pp. 94–105, 2014.

[10] I.-K. Park, J.-H. Kim, and K.-S. Hong, "An implementation of an fpga-based embedded gesture recognizer using a data glove," in *Proceedings of the 2nd international conference on Ubiquitous information management and communication*. ACM, 2008, pp. 496–500.

[11] C. Oz and M. C. Leu, "Recognition of finger spelling of american sign language with artificial neural network using position/orientation sensors and data glove," in *International Symposium on Neural Networks*. Springer, 2005, pp. 157–164.

[12] R. Ozawa and N. Ueda, "Supervisory control of a multi-fingered robotic hand system with data glove," in *2007 IEEE/RSJ International Conference on Intelligent Robots and Systems*. IEEE, 2007, pp. 1606–1611.

[13] A. Tognetti, N. Carbonaro, G. Zupone, and D. De Rossi, "Characterization of a novel data glove based on textile integrated sensors," in *2006 International Conference of the IEEE Engineering in Medicine and Biology Society*. IEEE, 2006, pp. 2510–2513.

[14] S. Pabon, E. Sotgiu, R. Leonardi, C. Brancolini, O. Portillo-Rodriguez, A. Frisoli, and M. Bergamasco, "A data-glove with vibro-tactile stimulators for virtual social interaction and rehabilitation," in *10th Annual Intl Workshop on Presence*, 2007, pp. 345–348.

[15] C.-S. Fahn and H. Sun, "Development of a data glove with reducing sensors based on magnetic induction," *IEEE Transactions on Industrial Electronics*, vol. 52, no. 2, pp. 585–594, 2005.

[16] P. Kumar, J. Verma, and S. Prasad, "Hand data glove: a wearable real-time device for human-computer interaction," *International Journal of Advanced Science and Technology*, vol. 43, 2012.

[17] G. Saggio, S. Bocchetti, C. A. Pinto, and G. Orengo, "Wireless data glove system developed for hmi," in *2010 3rd International Symposium on Applied Sciences in Biomedical and Communication Technologies (ISABEL 2010)*. IEEE, 2010, pp. 1–5.

[18] G. Saggio, F. Giannini, M. Todisco, and G. Costantini, "A data glove based sensor interface to expressively control musical processes," in *2011 4th IEEE International Workshop on Advances in Sensors and Interfaces (IWASI)*. IEEE, 2011, pp. 192–195.

[19] N. H. Adnan, K. Wan, A. Shahriman, S. K. Za'ba, H. Desa, and M. A. A. Aziz, "The development of a low cost data glove by using flexible bend sensor for resistive interfaces," in *The 2nd International Malaysia-Ireland Joint Symposium on Engineering, Science and Business*, 2012, pp. 579–587.

[20] A. Z. Shukor, M. F. Miskon, M. H. Jamaluddin, F. bin Ali, M. F. Asyraf, M. B. bin Bahar *et al.*, "A new data glove approach for malaysian sign language detection," *Procedia Computer Science*, vol. 76, pp. 60–67, 2015.

[21] J.-H. Kim, N. D. Thang, and T.-S. Kim, "3-d hand motion tracking and gesture recognition using a data glove," in *2009 IEEE International Symposium on Industrial Electronics*. IEEE, 2009, pp. 1013–1018.

[22] K. N. Tarchanidis and J. N. Lygouras, "Data glove with a force sensor," *IEEE Transactions on Instrumentation and Measurement*, vol. 52, no. 3, pp. 984–989, 2003.

[23] L. Lei and Q. Dashun, "Design of data-glove and chinese sign language recognition system based on arm9," in *2015 12th IEEE International Conference on Electronic Measurement & Instruments (ICEMI)*, vol. 3. IEEE, 2015, pp. 1130–1134.

[24] N. Tongrod, T. Kerdcharoen, N. Watthanawisuth, and A. Tuantranont, "A low-cost data-glove for human computer interaction based on ink-jet printed sensors and zigbee networks," in *International Symposium on Wearable Computers (ISWC) 2010*. IEEE, 2010, pp. 1–2.

[25] P.-C. Hsiao, S.-Y. Yang, B.-S. Lin, I.-J. Lee, and W. Chou, "Data glove embedded with 9-axis imu and force sensing sensors for evaluation of hand function," in *2015 37th annual international conference of the IEEE Engineering in Medicine and Biology Society (EMBC)*. IEEE, 2015, pp. 4631–4634.

[26] B. S. Lin, I. J. Lee, P. C. Hsiao, S. Y. Yang, and W. Chou, "Data glove embedded with 6-dof inertial sensors for hand rehabilitation," in *2014 Tenth International Conference on Intelligent Information Hiding and Multimedia Signal Processing*. IEEE, 2014, pp. 25–28.

[27] D. Lu, Y. Yu, and H. Liu, "Gesture recognition using data glove: An extreme learning machine method," in *2016 IEEE International Conference on Robotics and Biomimetics (ROBIO)*. IEEE, 2016, pp. 1349–1354.

[28] F. L. Hammond, Y. Mengüç, and R. J. Wood, "Toward a modular soft sensor-embedded glove for human hand motion and tactile pressure measurement," in *2014 IEEE/RSJ International Conference on Intelligent Robots and Systems*. IEEE, 2014, pp. 4000–4007.

[29] B. Fang, D. Guo, F. Sun, H. Liu, and Y. Wu, "A robotic hand-arm teleoperation system using human arm/hand with a novel data glove," in *2015 IEEE International Conference on Robotics and Biomimetics (ROBIO)*. IEEE, 2015, pp. 2483–2488.

[30] I. E. McDowall, M. T. Bolas, R. C. Mead Jr, and C. Greuel, "Virtual reality glove system with fabric conductors," Oct. 3 2000, uS Patent 6,128,004.

[31] L. K. Simone, N. Sundarrajan, X. Luo, Y. Jia, and D. G. Kamper, "A low cost instrumented glove for extended monitoring and functional hand assessment," *Journal of neuroscience methods*, vol. 160, no. 2, pp. 335–348, 2007.

[32] Z. Shen, J. Yi, X. Li, M. H. P. Lo, M. Z. Chen, Y. Hu, and Z. Wang, "A soft stretchable bending sensor and data glove applications," *Robotics and biomimetics*, vol. 3, no. 1, p. 22, 2016.

[33] Y. Li, X. Miao, and R. K. Raji, "Flexible knitted sensing device for identifying knee joint motion patterns," *Smart Materials and Structures*, vol. 28, no. 11, p. 115042, 2019.

[34] S. Seyedin, J. M. Razal, P. C. Innis, A. Jeiranikhameneh, S. Beirne, and G. G. Wallace, "Knitted strain sensor textiles of highly conductive all-polymeric fibers," *ACS applied materials & interfaces*, vol. 7, no. 38, pp. 21 150–21 158, 2015.

[35] O. Atalay, W. R. Kennon, and E. Demirok, "Weft-knitted strain sensor for monitoring respiratory rate and its electro-mechanical modeling," *IEEE Sensors Journal*, vol. 15, no. 1, pp. 110–122, 2015.
[36] R. Postle and D. Munden, "Analysis of the dry-relaxed knitted-loop configuration: Part i: Two-dimensional analysis," *Journal of the Textile Institute*, vol. 58, no. 8, pp. 329–351, 1967.
[37] D. J. Spencer, *Knitting technology: a comprehensive handbook and practical guide*. CRC press, 2001, vol. 16.
[38] L. Li, W. M. Au, T. Hua, and K. S. Wong, "Design of a conductive fabric network by the sheet resistance method," *Textile research journal*, vol. 81, no. 15, pp. 1568–1577, 2011.
[39] L. Li, W. M. Au, K. M. Wan, S. H. Wan, W. Y. Chung, and K. S. Wong, "A resistive network model for conductive knitting stitches," *Textile research journal*, vol. 80, no. 10, pp. 935–947, 2010.
[40] L. Li, S. Liu, F. Ding, T. Hua, W. M. Au, and K.-S. Wong, "Electromechanical analysis of length-related resistance and contact resistance of conductive knitted fabrics," *Textile research journal*, vol. 82, no. 20, pp. 2062–2070, 2012.
[41] H. Zhang and X. Tao, "From wearable to aware: Intrinsically conductive electrotextiles for human strain/stress sensing," in *Biomedical and Health Informatics (BHI), 2012 IEEE-EMBS International Conference on*. IEEE, 2012, pp. 468–471.
[42] H. Zhang, X. Tao, S. Wang, and T. Yu, "Electro-mechanical properties of knitted fabric made from conductive multi-filament yarn under unidirectional extension," *Textile research journal*, vol. 75, no. 8, pp. 598–606, 2005.
[43] C. Isaia, D. S. McNally, S. A. McMaster, and D. T. Branson, "Effect of mechanical preconditioning on the electrical properties of knitted conductive textiles during cyclic loading," *Textile Research Journal*, vol. 89, no. 3, pp. 445–460, 2019.
[44] O. Atalay, W. R. Kennon, and M. D. Husain, "Textile-based weft knitted strain sensors: Effect of fabric parameters on sensor properties," *Sensors*, vol. 13, no. 8, pp. 11 114–11 127, 2013.
[45] O. Atalay and W. Kennon, "Knitted strain sensors: Impact of design parameters on sensing properties," *Sensors*, vol. 14, no. 3, pp. 4712–4730, 2014.
[46] F. T. Peirce, "Geometrical principles applicable to the design of functional fabrics," *Textile Research Journal*, vol. 17, no. 3, pp. 123–147, 1947.
[47] C. M. Bishop, *Pattern recognition and machine learning*. springer, 2006.
[48] N. Lv, X. Yang, Y. Jiang, and T. Xu, "Sparse decomposition for data glove gesture recognition," in *2017 10th International Congress on Image and Signal Processing, BioMedical Engineering and Informatics (CISP-BMEI)*. IEEE, 2017, pp. 1–5.
[49] P. D. Rosero-Montalvo, P. Godoy-Trujillo, E. Flores-Bosmediano, J. Carrascal-García, S. Otero-Potosi, H. Benitez-Pereira, and D. H. Peluffo-Ordóñez, "Sign language recognition based on intelligent glove using machine learning techniques," in *2018 IEEE Third Ecuador Technical Chapters Meeting (ETCM)*. IEEE, 2018, pp. 1–5.